

Improving Variable-Length Generation in Diffusion Language Models via Length Regularization

Zicong Cheng¹ Ruixuan Jia¹ Jia Li¹ Guo-Wei Yang² Meng-Hao Guo¹ Shi-Min Hu¹

Abstract

Diffusion Large Language Models (DLLMs) are inherently ill-suited for variable-length generation, as their inference is defined on a fixed-length canvas and implicitly assumes a known target length. When the length is unknown, as in realistic completion and infilling, naively comparing confidence across mask lengths becomes systematically biased, leading to under-generation or redundant continuations. In this paper, we show that this failure arises from an intrinsic length-induced bias in generation confidence estimates, leaving existing DLLMs without a robust way to determine generation length and making variable-length inference unreliable. To address this issue, we propose LR-DLLM, a length-regularized inference framework for DLLMs that treats generation length as an explicit variable and achieves reliable length determination at inference time. It decouples semantic compatibility from length-induced uncertainty through an explicit length regularization that corrects biased confidence estimates. Based on this, LR-DLLM enables dynamic expansion or contraction of the generation span without modifying the underlying DLLM or its training procedure. Experiments show that LR-DLLM achieves **51.3%** Pass@1 on HumanEval-Infilling under fully unknown lengths (**+13.4%** vs. DreamOn) and **51.5%** average Pass@1 on four-language McEval (**+14.3%** vs. DreamOn).

1. Introduction

DLLMs are emerging as a promising alternative to autoregressive language models (Xie et al., 2025; Nie et al., 2025; Zhu et al., 2025a; Bie et al., 2025), offering a different generation paradigm based on bidirectional denoising over a fixed-length canvas, rather than left-to-right factorization. In particular, DLLMs are well suited for conditional genera-

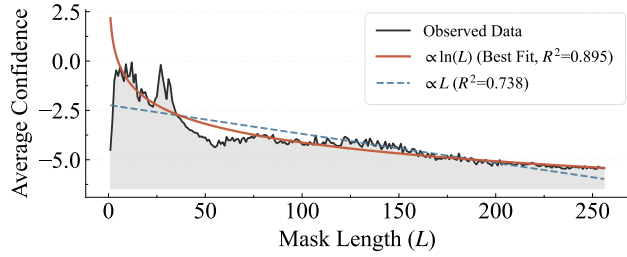


Figure 1. Average confidence as a function of mask length L (log-scaled x-axis). The observed trend is well characterized by a logarithmic dependence ($\propto \log L$), while a linear fit provides a noticeably poorer approximation.

tion scenarios such as fill-in-the-middle (FIM), where both prefix and suffix context are available. However, despite these advantages, popular DLLMs remain fundamentally designed for fixed-length generation, implicitly assuming that the target span length is known in advance.

This assumption is frequently violated in realistic settings. In practical completion and infilling tasks, the length of the missing span is often unknown and variable, and forcing inference to operate on a pre-fixed canvas can lead to systematic failures. When the chosen length is shorter than required, DLLMs tend to under-generate, producing incomplete or semantically invalid outputs; when the length is overestimated, they exhibit redundant continuations. Therefore, variable-length generation remains a critical bottleneck that limits the applicability of DLLMs in real-world scenarios.

Existing attempts at variable-length generation in DLLMs can be broadly divided into training-based and training-free approaches, yet both suffer from limitations for solving this challenge. On the one hand, training-based methods typically introduce specialized objectives or auxiliary components, which require additional retraining and interfere with the model’s original language modeling capability. On the other hand, training-free approaches are typically more lightweight, but often rely on special control tokens or only allow one-sided adjustments, which restrict flexibility (Li et al., 2025). As a result, current solutions still fall short of being simultaneously training-free, model-agnostic, and task-agnostic (Table 1). In this paper, we focus on developing a training-free variable-length generation that preserves model

¹Tsinghua University ²Proxseer Inc..

Table 1. Comparison of key properties across variable-length generation methods. ([†] Task-agnostic here refers to the ability to support both fill-in-the-middle (FIM) and standard left-to-right completion.)

Method	Training-free	Model-agnostic	Task-agnostic [†]	GSM8K
DAEDAL	✓	✗	✗	63.3
DreamOn	✗	✗	✓	-
FlexMDM	✗	✗	✓	67.0
dLLM-Var	✗	✗	✗	70.9
LR-DLLM	✓	✓	✓	75.1

generality while enabling flexible length adaptation.

We propose LR-DLLM, a training-free framework for dynamic variable-length decoding in diffusion LLMs that treats generation length as an explicit inference variable. Rather than fixing the canvas length *a priori*, LR-DLLM probes candidate lengths and leverages the model’s own generation confidence to search for a more appropriate length. Specifically, it first evaluates a small set of exponentially spaced candidate lengths (e.g., $L \in \{1, 2, 4, 8, \dots\}$) and selects the one maximizing the calibrated confidence as an initial guess. Starting from this initialization, the framework greedily expands or contracts the generation span in a bidirectional manner, guided solely by confidence feedback from the underlying DLLM. The entire procedure operates at inference time and requires no retraining or architectural modification, making it directly applicable to existing diffusion backbones.

A key challenge is comparing confidence across different lengths. Naively selecting the length with the highest average confidence fails due to an intrinsic length-induced bias in DLLMs: confidence drifts approximately logarithmically with canvas length, independent of semantic compatibility. As a result, raw confidence conflates semantic fit with length-dependent uncertainty. We address this by introducing a $\log L$ regularizer that corrects for length bias, yielding a calibrated confidence-length criterion. The regularization coefficient is estimated via lightweight probing, enabling reliable cross-length comparison and robust bidirectional length adjustment during inference.

Experiments show that LR-DLLM achieves 51.3% Pass@1 on HumanEval-Infilling with unknown lengths (+13.4% over DreamOn) and 51.5% average Pass@1 on the four-language McEval benchmark (+14.3%), highlighting its strong generality across models and tasks.

In summary, our key contributions are:

- We identify an intrinsic *length-induced bias* in DLLM confidence estimates, demonstrating that naive confidence comparisons across lengths are unreliable for unknown-length generation.
- We introduce a length-regularized criterion incorporating a $\log L$ term, providing a principled signal for

scoring candidate lengths at inference time.

- We propose LR-DLLM, a training-free inference framework that leverages this criterion via efficient probing and greedy bidirectional adjustment, validating its superiority across diverse benchmarks.

2. Preliminary and Notation

2.1. Preliminary

We study conditional generation problems in which the output must satisfy a hard context constraint, but the number of tokens to be generated is not specified. Given an observed context \mathbf{c} , the goal is to generate a token span $\mathbf{y} \in \mathcal{V}^*$ of unknown length and form a completed sequence $\mathbf{x} = g(\mathbf{c}, \mathbf{y})$ that respects the constraint induced by \mathbf{c} , where $g(\cdot, \cdot)$ is a deterministic, task-specific composition function. As a simple example, infilling corresponds to a prefix-suffix context $\mathbf{c} = (\mathbf{p}, \mathbf{s})$ with completion $\mathbf{x} = \mathbf{p} \parallel \mathbf{y} \parallel \mathbf{s}$. We denote the (unknown) target span length by $L^* := |\mathbf{y}|$.

2.2. Notation

Table 2 summarizes the notation used throughout the paper.

Table 2. Notation used in the paper.

Symbol	Description
\mathcal{V}	Vocabulary
$\mathbf{x} = (x_1, \dots, x_T)$	Token sequence of length T
$ \mathbf{x} $	Length of sequence \mathbf{x}
$\mathbf{a} \parallel \mathbf{b}$	Concatenation of two sequences
$\langle \text{mask} \rangle$	Special mask token
$\langle \text{mask} \rangle^L$	Mask block of length L
\mathbf{p}, \mathbf{s}	Prefix and suffix context
\mathbf{y}	Generated token span
L^*	(Unknown) target span length, $L^* = \mathbf{y} $

3. LR-DLLM

LR-DLLM is a training-free method for variable-length generation. Unlike standard DLLM, which assumes a fixed mask length, the target span length under prefix-suffix constraints is unknown. LR-DLLM resolves it by modeling span length as an *inference-time variable*. It relies on a length-confidence signal derived from the model’s uncertainty estimates to guide length selection. Using this signal, LR-DLLM combines a lightweight probing-based initialization with inference-time refinement for the precise length.

3.1. Overview

Given a prefix-suffix context (\mathbf{p}, \mathbf{s}) , LR-DLLM performs variable-length generation by explicitly treating the remaining span length as an inference-time decision variable. Crucially, this requires correcting the intrinsic bias of confidence

estimates with respect to length; without explicit length regularization, confidence scores across different candidate lengths are not directly comparable, making reliable length selection impossible.

At each step, LR-DLLM uses the proposed length-confidence signal to determine (i) how much content remains to be generated and (ii) when it is appropriate to commit a new token. Overall, LR-DLLM consists of two stages:

- **Stage I (Initialization by probing).** A small set of candidate lengths is probed to estimate an instance-specific length regularization coefficient and to select an initial remaining length that is calibrated to the given context.
- **Stage II (Inference-time refinement).** During generation, the remaining length is locally refined using the length-regularized confidence signal. A token is committed once the current length becomes locally preferred under this criterion. This process repeats until the span is fully generated or a global budget is reached.

3.2. Length-Confidence Signal

To select an appropriate masked span length during inference, we require a scalar signal that allows us to *compare different candidate lengths under the same prefix-suffix context*. A natural choice is to measure how confidently the model can fill a masked block of a given length. In this subsection, we formalize such a confidence measure and show how to correct it for a systematic length-induced bias.

Span-level confidence from token uncertainty. Let $\mathbf{c} = (\mathbf{p}, \mathbf{s})$ denote the prefix-suffix context, and let $q_\theta(\cdot | \mathbf{x}, \mathbf{c})$ be the token distribution produced by the DLLM inference procedure for a masked position. We quantify the confidence at a masked position i using the negative entropy of this distribution:

$$\text{conf}(i; \mathbf{x}, \mathbf{c}) := \sum_{v \in \mathcal{V}} q_\theta(v | \mathbf{x}, \mathbf{c}) \log q_\theta(v | \mathbf{x}, \mathbf{c}). \quad (1)$$

Intuitively, a lower-entropy distribution indicates that the model is more certain about the token to be generated at that position.

Given a length- L masked template $\mathbf{x}^{(0)}(L) = \mathbf{p} \parallel \langle \text{mask} \rangle^L \parallel \mathbf{s}$, we aggregate the token-level confidences over the L masked positions and define the span-level confidence as their average:

$$\text{AVG}_{\text{conf}}(L; \mathbf{p}, \mathbf{s}) := \frac{1}{L} \sum_{i \in \mathcal{M}(L)} \text{conf}(i; \mathbf{x}, \mathbf{c}), \quad (2)$$

where $\mathcal{M}(L)$ denotes the index set of the masked block. In practice, all masked token distributions required to com-

pute $\text{AVG}_{\text{conf}}(L; \mathbf{p}, \mathbf{s})$ are obtained from a single standard inference pass of the underlying diffusion model.

Length-confounded confidence. The quantity $\text{AVG}_{\text{conf}}(L; \mathbf{p}, \mathbf{s})$ varies with the mask length L for two distinct reasons. On the one hand, it reflects whether a span of length L is semantically compatible with the given prefix and suffix. On the other hand, it is systematically influenced by the number of masked positions itself, because changing L alters the uncertainty structure of masked prediction even under an identical context. To disentangle these effects, we model the observed span-level confidence as

$$\text{AVG}_{\text{conf}}(L; \mathbf{p}, \mathbf{s}) = S(L; \mathbf{p}, \mathbf{s}) + R(L; \mathbf{p}, \mathbf{s}), \quad (3)$$

where $S(L; \mathbf{p}, \mathbf{s})$ captures the context-length compatibility that we seek to evaluate, and $R(L; \mathbf{p}, \mathbf{s})$ represents a systematic shift induced by length.

Length-confidence signal. While $S(L; \mathbf{p}, \mathbf{s})$ is not directly observable, the aggregate confidence $\text{AVG}_{\text{conf}}(L; \mathbf{p}, \mathbf{s})$ is. We therefore estimate and subtract the length-induced bias term $R(L; \mathbf{p}, \mathbf{s})$. As shown in Appendix E, under mild assumptions this bias admits a logarithmic form $R(L; \mathbf{p}, \mathbf{s}) = k \log L$, where the coefficient k is instance-dependent and may vary across contexts. This yields our length-confidence signal:

$$\text{CL}(L; \mathbf{p}, \mathbf{s}) := \text{AVG}_{\text{conf}}(L; \mathbf{p}, \mathbf{s}) - k \log L, \quad (4)$$

which removes the systematic length effect from the raw confidence score. The resulting signal serves as a practical proxy for the semantic compatibility $S(L; \mathbf{p}, \mathbf{s})$ and enables direct comparison between candidate lengths. In the following subsections, we describe how LR-DLLM estimates the coefficient k and selects an initial length (Stage I), and how it performs greedy bidirectional length adjustment during inference (Stage II).

3.3. Stage I: Parameter Estimation and Length Selection

Our length-confidence signal is $\text{CL}(L; \mathbf{p}, \mathbf{s}) = \text{AVG}_{\text{conf}}(L; \mathbf{p}, \mathbf{s}) - k \log L$. In deployment, the coefficient k is previously unknown and may vary between instances. Stage I therefore performs two tasks: First, it estimates an instance-specific \hat{k} with a small number of probes, and then selects an initialization length L_{rem} that is already adapted to the given context. The full procedure is provided in Algorithm 1.

Exponential probing of candidate lengths. Given a maximum probing length `MAX_LENGTH`, we probe a compact set of exponentially spaced lengths $\mathcal{L}_{\text{exp}} = \{1, 2, 4, \dots, 2^m\}$ where $2^m \leq \text{MAX_LENGTH}$. For each $L \in \mathcal{L}_{\text{exp}}$, we

4. Experiment

In this section, we conduct extensive experiments to demonstrate that LR-DLLM exhibits strong generalization across models and broad applicability across tasks. Our empirical study is organized around the following research questions:

- **RQ1:** How does LR-DLLM perform on infilling tasks?
- **RQ2:** How well does LR-DLLM generalize across different programming languages for infilling?
- **RQ3:** How well does LR-DLLM generalize to general-purpose benchmarks beyond infilling?
- **RQ4:** What is the impact of the $\log L$ regularization term on the performance of LR-DLLM?
- **RQ5:** What is the contribution of Stage II to the overall effectiveness of LR-DLLM?

4.1. Experimental Settings

Datasets. We evaluate LR-DLLM on both code infilling and general-purpose reasoning tasks. For infilling, we use HumanEval-Infilling (Bavarian et al., 2022). To assess multilingual infill robustness, we additionally adopt McEval (Chai et al., 2025), covering four programming languages: C++, Python, JavaScript, and Rust. For general-purpose evaluation, we consider HumanEval (Yadav & Mondal, 2025) for code generation, GSM8K (Cobbe et al., 2021) and MATH500 (Lightman et al., 2024) for math reasoning.

Models. For code infilling, we test representative diffusion-based code models, including LLaDA-8B (Nie et al., 2025), LLaDA-1.5 (Zhu et al., 2025a), LLaDA-MoE-7B (Zhu et al., 2025b), Dream (Ye et al., 2025), and DreamCoder (Xie et al., 2025). For general-purpose benchmarks, we evaluate the subset of these models that are trained or tuned for broader instruction-following and reasoning capabilities.

Baselines. On fill-in-the-middle (FIM) infilling, we compare against two training-based variable-length approaches, DreamOn (Wu et al., 2025) and FlexMDM (Kim et al., 2025). For general-purpose tasks, we include DAEDAL (Li et al., 2025) as a representative training-free baseline.

Metrics. For coding-related tasks (including infilling and code generation), we report Pass@1. For GSM8K and MATH500, we use accuracy as evaluation metric.

4.2. Main Results on Code Infilling (RQ1)

Table 3 presents the main results on HumanEval-Infilling. Unless otherwise specified, the *Baseline* infills with a fixed length of 64 [MASK] tokens, whereas all variable-length methods (including LR-DLLM, DreamOn, and FlexMDM) are evaluated under the same adjustment budget with `MAX_LENGTH=128`, allowing automatic expansion and contraction during inference. Under this controlled comparison,

LR-DLLM yields consistent improvements across every backbone, indicating strong model-agnostic generalization.

On average, LR-DLLM substantially increases mean Pass@1 across models, despite their very different starting points. For LLaDA-8B, the mean rises from 23.4 to 36.7, corresponding to a 56.8% relative improvement; for LLaDA-1.5, it improves from 31.2 to 36.1, a 15.7% gain. LLaDA-MoE increases from 35.1 to 40.8, a 16.2% gain, while the Dream-family models benefit even more: Dream-7B jumps from 22.5 to 44.8, nearly doubling performance with a 99.1% relative improvement, and DreamCoder-7B increases from 39.1 to 51.3, a 31.2% gain. The fact that LR-DLLM improves both weaker and stronger backbones suggests that the proposed inference mechanism provides broadly useful inductive bias rather than exploiting model-specific quirks.

The gains concentrate on the most length-sensitive regime, namely Multi-line infilling, where fixed masking frequently leads to under-generation or redundant continuations. Across models, LR-DLLM yields the largest improvements in this setting, with consistent gains also observed for Single-line infilling. These trends directly validate the core design of LR-DLLM: by treating span length as an explicit inference variable and enabling bidirectional length adjustment, the method mitigates both semantic gaps and redundancy when the target length is unknown.

LR-DLLM further demonstrates improved reliability over existing variable-length baselines. On DreamCoder-7B, the training-based DreamOn exhibits inconsistent behavior across span regimes, improving some settings while degrading Multi-line infilling. In contrast, LR-DLLM consistently improves Random Span, Single-line, and Multi-line infilling simultaneously, resulting in the strongest overall performance. This uniform gain across heterogeneous span lengths indicates more robust length selection, achieved by explicitly correcting length-induced confidence bias rather than relying on heuristic or initialization-dependent length priors.

Overall, these results show that LR-DLLM consistently delivers large and robust gains, especially on long and challenging infilling instances. Importantly, these improvements are achieved with a modest inference-time overhead: while LR-DLLM performs local probing and bidirectional adjustment, the average number of additional forward calls per generated token remains small and bounded across benchmarks (Table 9). This indicates that LR-DLLM effectively optimizes the generation span with an approximately constant average cost, rather than incurring unbounded or length-proportional overhead.

Table 3. HumanEval-Infilling (Pass@1). Within each backbone, **bold** denotes the best score in the corresponding column. Shaded cells indicate results obtained by LR-DLLM on the same backbone. Mean is averaged over Random Span, Single-line, and Multi-line. For DreamOn, we set the initial mask length to 1 to isolate its variable-length adjustment capability.

Model	Method	HumanEval-Infilling (Pass@1)			
		Random Span	Single-line	Multi-line	Mean
LLaDA-8B	Baseline	16.0	48.3	21.1	23.4
	+FlexMDM	—	65.0	—	—
	+LR-DLLM	19.1	69.4	35.9	36.7
LLaDA-1.5	Baseline	16.5	48.8	32.2	31.2
	+LR-DLLM	20.5	68.9	34.6	36.1
LLaDA-MoE	Baseline	14.6	48.8	38.4	35.1
	+LR-DLLM	21.5	71.3	41.4	40.8
Dream-7B	Baseline	8.17	48.2	21.9	22.5
	+LR-DLLM	19.6	76.7	46.3	44.8
DreamCoder-7B	Baseline	14.3	55.5	43.2	39.1
	+DreamOn	21.6	73.5	36.1	37.9
	+LR-DLLM	23.2	81.6	53.8	51.3

4.3. Cross-Language Generalization for Infilling (RQ2)

Table 4 evaluates cross-language infilling on McEval. Unless otherwise specified, the *Baseline* fills a fixed span of 32 [MASK] tokens, while all variable-length methods (including LR-DLLM and DreamOn) use the same adjustment budget with `MAX_LENGTH=256`, enabling automatic expansion and contraction at inference time. Within this unified setting, LR-DLLM consistently improves performance across all four languages and for both Single-line and Multi-line infilling, demonstrating strong cross-language generalization without language-specific tuning.

Averaged over languages and settings, LR-DLLM delivers sizable relative gains on every diffusion backbone. The mean score of LLaDA-8B increases from 37.0 to 44.2, corresponding to a relative improvement of 19.5%; LLaDA-MoE rises from 41.0 to 51.8, a 26.3% gain; Dream-7B improves from 35.8 to 47.9, yielding a 33.8% gain; and DreamCoder-7B jumps from 37.2 to 51.5, which translates to a 38.4% gain. Although the absolute baseline performance varies substantially across models, LR-DLLM consistently provides strong improvements, indicating that our length-aware inference mechanism is not tied to a particular backbone or training recipe.

The gains are especially pronounced on the Multi-line setting, where fixed masking most frequently causes length mismatch. For instance, on LLaDA-MoE, Multi-line accuracy more than doubles across multiple languages: JavaScript increases from 12.5 to 28.8, improving by 130.4%; Python rises from 11.1 to 26.7, improving by 140.5%; and Rust climbs from 7.61 to 25.0, improving by 228.5%. Dream-7B shows the same trend, with Multi-line improving by 93.1% on JavaScript (17.5 to 33.8) and by 162.4% on Python (8.88 to

23.3). These consistent, large relative gains on Multi-line support our central claim: explicitly optimizing span length via bidirectional adjustment is critical for robust infilling when the missing span length is unknown.

Compared with the training-based DreamOn baseline, LR-DLLM is also markedly more robust under cross-language shift. On DreamCoder-7B, DreamOn yields uneven transfer: while it improves Python, it significantly degrades Single-line performance on C++ from 57.3 to 39.1 and on Rust from 52.2 to 27.2, leaving the overall mean unchanged at 37.2. In contrast, LR-DLLM improves DreamCoder-7B consistently across all languages and settings, including large Multi-line gains such as JavaScript from 12.5 to 38.8 (a 210.4% increase) and Rust from 6.52 to 21.7 (a 232.8% increase). This suggests that LR-DLLM provides a more stable, model-agnostic way to handle length uncertainty than methods that rely on training-time heuristics.

4.4. Results on General-Purpose Benchmarks (RQ3)

Table 5 reports results on GSM8K, HumanEval, and MATH500. We compare fixed-length generation with different mask lengths $L \in \{32, 64, 128\}$, DAEDAL initialized with $L=1$, and LR-DLLM under the same diffusion backbones. Overall, LR-DLLM consistently improves over fixed-length decoding across tasks and models, and it also surpasses DAEDAL on the LLaDA backbones where DAEDAL is applicable.

The most significant gains appear on MATH500. On LLaDA-8B, LR-DLLM raises MATH500 from 26.4 to 39.8, a 50.8% relative improvement over DAEDAL, and it also improves GSM8K from 63.3 to 75.1 by 18.6%. On LLaDA-1.5, LR-DLLM boosts MATH500 from 24.0 to 38.6, achieving

Table 4. Multilingual code infilling results. Pass@1 (%) on Single-line and Multi-line infilling across four programming languages (JavaScript, Python, C++, and Rust). Within each backbone, **bold** denotes the best score in the corresponding column. Shaded cells indicate results obtained by applying LR-DLLM to the same backbone. **Mean** is the sample-size-weighted average over the eight language-setting columns. For DreamOn, we set the initial mask length to 1.

Model	Method	JavaScript		Python		C++		Rust		Mean
		Single	Multi	Single	Multi	Single	Multi	Single	Multi	
Diffusion Models										
LLaDA-8B	Baseline	62.5	16.3	68.9	10.0	57.3	23.1	51.1	7.61	37.0
LLaDA-8B	+LR-DLLM	68.8	27.5	70.0	22.0	68.3	25.6	60.9	12.0	44.2
LLaDA-MoE	Baseline	62.5	12.5	84.4	11.1	61.0	31.7	57.6	7.61	41.0
LLaDA-MoE	+LR-DLLM	76.3	28.8	85.6	26.7	75.6	32.9	64.1	25.0	51.8
Dream-7B	Baseline	53.8	17.5	66.7	8.88	61.0	13.4	39.1	8.70	35.8
Dream-7B	+LR-DLLM	75.0	33.8	72.2	23.3	82.9	24.4	59.8	14.1	47.9
DreamCoder-7B	Baseline	66.3	12.5	73.3	10.0	57.3	20.7	52.2	6.52	37.2
DreamCoder-7B	+DreamOn	62.5	18.8	82.2	23.3	39.1	15.9	27.2	7.60	37.2
DreamCoder-7B	+LR-DLLM	78.8	38.8	77.8	30.0	76.8	28.0	62.0	21.7	51.5
Autoregressive (AR) Models										
DeepSeek-Coder-6.7B	Baseline	64.0	40.0	66.0	32.4	60.0	33.8	54.7	33.2	47.9

Table 5. We compare fixed-length generation with different mask lengths ($L \in \{32, 64, 128\}$), DAEDAL with initial $L=1$, and LR-DLLM under the same backbones. “–” denotes results not available (the method is not applicable or not reported).

Benchmark	Fixed-Length			DAEDAL	LR-DLLM
	32	64	128		
LLADA-8B					
GSM8K	40.2	48.0	67.9	63.3	75.1
HumanEval	12.2	18.9	26.2	27.4	31.7
MATH500	22.6	22.6	23.6	26.4	39.8
LLADA-1.5					
GSM8K	41.2	49.4	71.0	66.5	76.7
HumanEval	16.5	18.3	22.0	32.3	34.8
MATH500	24.0	22.0	23.4	24.0	38.6
Dream-7B					
GSM8K	24.0	52.7	75.9	–	76.6
HumanEval	12.8	25.9	48.3	–	53.6
MATH500	14.2	24.2	38.6	–	41.4

a 60.8% relative improvement, while increasing GSM8K from 66.5 to 76.7 by 15.3%. These results suggest that explicit length optimization is especially beneficial for math-intensive reasoning, where suboptimal length often manifests as incomplete derivations or redundant steps.

DAEDAL cannot be applied to non-LLADA diffusion backbones, so no DAEDAL results are reported for Dream-7B. Nevertheless, LR-DLLM still delivers striking improvements over the best fixed-length setting on Dream-7B, most notably on HumanEval, where performance jumps from 48.3 at $L=128$ to 53.6, a 11.0% relative gain, and on MATH500, where it increases from 38.6 to 41.4, a 7.3% relative gain.

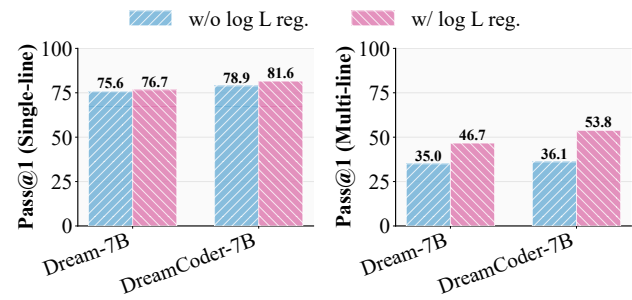


Figure 2. Ablation of the $\log L$ regularization term in LR-DLLM on HumanEval-Infilling (Pass@1). All methods use the same length adjustment budget with $\text{MAX_LENGTH}=128$.

Meanwhile, GSM8K remains essentially unchanged, with LR-DLLM achieving 76.6 compared with the best fixed-length result of 75.9, indicating that LR-DLLM can preserve strong performance on less length-sensitive benchmarks while substantially improving the most length-critical ones.

4.5. Ablation on $\log L$ Regularization (RQ4)

Fig. 2 ablates the $\log L$ regularization term in LR-DLLM on HumanEval-Infilling. Introducing $\log L$ regularization yields consistent gains across both backbones, and the improvements are notably larger in the Multi-line setting, which is more sensitive to length ambiguity. In contrast, Single-line shows smaller but still positive changes, suggesting that when the target span is short and well constrained, length selection is less of a bottleneck.

Qualitatively, these trends align with the role of the $\log L$ term as an explicit complexity penalty during inference: it discourages unnecessarily long candidate spans, thereby

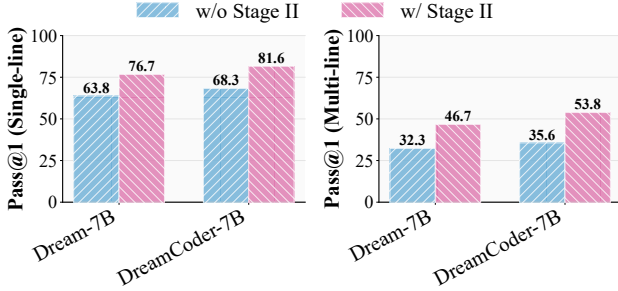


Figure 3. Effect of Stage II (mid-span adjustment) in LR-DLLM on HumanEval-Infilling (Pass@1) for Dream-7B and DreamCoder-7B.

reducing redundant continuation and helping the model commit to a more coherent span that better matches the prefix–suffix context. This effect becomes most pronounced for Multi-line infilling, where the search space over plausible lengths is widest and naive confidence-based selection is most prone to over-generation.

4.6. Ablation on Stage II (RQ5)

Fig. 3 ablates Stage II (mid-span adjustment) in LR-DLLM on HumanEval-Infilling. Across both backbones, enabling Stage II yields substantial and consistent gains, with the improvements most pronounced on Multi-line, where failures often arise from local inconsistencies inside long spans (e.g., drifting variables, broken control flow, or mismatched intermediate states) rather than only boundary length mismatch. On Dream-7B, Stage II increases Single-line Pass@1 from 63.8 to 76.7 (+12.9; +20.2% relative) and boosts Multi-line from 32.3 to 46.7 (+14.4; +44.6% relative). A similar pattern holds for DreamCoder-7B: Single-line rises from 68.3 to 81.6 (+13.3; +19.5% relative), and Multi-line increases from 35.6 to 53.8 (+18.2; +51.1% relative).

These trends suggest that Stage II contributes more than coarse length correction: it actively refines the span interior, fixing mid-span errors that would otherwise persist even when the overall length is plausible. As a result, LR-DLLM achieves markedly better Multi-line coherence, indicating that mid-span refinement is a crucial complement to Stage I’s boundary-driven length adjustment.

5. Related Work

5.1. Variable-Length Generation in Diffusion Large Language Models (DLLMs)

Unlike autoregressive models (Guo et al., 2025; Yang et al., 2025a; Zhang et al., 2025b), most DLLMs assume a *fixed*-length canvas, which conflicts with variable-length FIM. Current methods are either *training-based* or *training-free*.

Training-based methods. DreamOn trains special edit tokens (e.g., `<expand>`, `<delete>`) and applies custom inference rules to insert or remove masked positions (Wu et al., 2025). AnyOrder redesigns denoising to jointly predict tokens and inter-token mask counts for flexible length (Kim et al., 2025). Flexible changes token positions during generation to adjust the number of masks, also requiring training-time modifications (Zhang et al., 2025a). DLLM-var is another training-based approach that relies on explicit termination signals (e.g., EOS-style stopping) for variable-length generation (Yang et al., 2025b), which is less convenient for arbitrary-span FIM or settings without a clear EOS boundary. Overall, these methods improve flexibility but incur extra training cost and may reduce compatibility with strong off-the-shelf DLLMs. In contrast, LR-DLLM is training-free and preserves the original DLLM denoising rule while enabling stable bidirectional length adjustment.

Training-free methods. Beyond-Fixed studies training-free variable-length generation via inference-time heuristics for selecting or adjusting the length canvas (Li et al., 2025). While avoiding retraining, such heuristics can be sensitive to initialization and brittle under large length variance in FIM. LR-DLLM is also training-free, but treats length as an explicit inference variable and supports both expansion and contraction, reducing sensitivity to the initial mask length.

5.2. Diffusion Large Language Models (DLLMs)

DLLMs conduct iterative denoising with bidirectional context and have recently shown strong performance on general and code generation. Representative large-scale DLLMs include the LLADA family (Nie et al., 2025; Zhu et al., 2025a;b), DEER (Cheng et al., 2025) and Dream (Ye et al., 2025). However, most DLLM inference pipelines remain fixed-length, which restricts their applicability to realistic FIM and completion where output length is not given. Our work complements these DLLMs by enabling variable-length inference without modifying or retraining the underlying model, making existing DLLMs directly usable in unknown-length constrained generation.

6. Conclusion

We presented LR-DLLM, a training-free framework for unknown-length constrained generation in diffusion LLMs. By treating length as an explicit inference variable and optimizing a debiased length–confidence signal, LR-DLLM supports bidirectional length adjustment (expansion and contraction) without modifying the base model. Beyond infilling, we evaluate LR-DLLM on general-purpose benchmarks (MATH500, GSM8K, and HumanEval), demonstrating that it also improves standard left-to-right generation.

7. Impact Statement

This paper presents work whose goal is to advance the field of machine learning. There are many potential societal consequences of our work, none of which we feel must be specifically highlighted here.

References

Bavarian, M., Jun, H., Tezak, N., Schulman, J., McLeavey, C., Tworek, J., and Chen, M. Efficient training of language models to fill in the middle. *CoRR*, abs/2207.14255, 2022.

Bie, T., Cao, M., Chen, K., Du, L., Gong, M., Gong, Z., Gu, Y., Hu, J., Huang, Z., Lan, Z., Li, C., Li, C., Li, J., Li, Z., Liu, H., Liu, L., Lu, G., Lu, X., Ma, Y., Tan, J., Wei, L., Wen, J.-R., Xing, Y., Zhang, X., Zhao, J., Zheng, D., Zhou, J., Zhou, J., Zhou, Z., Zhu, L., and Zhuang, Y. Llada2.0: Scaling up diffusion language models to 100b, 2025. URL <https://arxiv.org/abs/2512.15745>.

Chai, L., Liu, S., Yang, J., Yin, Y., Jin, K., Liu, J., Sun, T., Zhang, G., Ren, C., Guo, H., Wang, N., Wang, B., Wu, X., Wang, B., Li, T., Yang, L., Duan, S., Zhang, Z., and Li, Z. Mceval: Massively multilingual code evaluation. In *The Thirteenth International Conference on Learning Representations, ICLR 2025, Singapore, April 24-28, 2025*. OpenReview.net, 2025.

Chen, X., Huang, S., Guo, C., Wei, C., He, Y., Zhang, J., Li, H. H., and Chen, Y. Dpad: Efficient diffusion language models with suffix dropout. *CoRR*, abs/2508.14148, 2025.

Cheng, Z., Yang, G.-W., Li, J., Deng, Z., Guo, M.-H., and Hu, S.-M. Deer: Draft with diffusion, verify with autoregressive models. *arXiv preprint arXiv:2512.15176*, 2025.

Cobbe, K., Kosaraju, V., Bavarian, M., Chen, M., Jun, H., Kaiser, L., Plappert, M., Tworek, J., Hilton, J., Nakano, R., Hesse, C., and Schulman, J. Training verifiers to solve math word problems. *CoRR*, abs/2110.14168, 2021.

Feng, G., Geng, Y., Guan, J., Wu, W., Wang, L., and He, D. Theoretical benefit and limitation of diffusion language model. *CoRR*, abs/2502.09622, 2025. doi: 10.48550/ARXIV.2502.09622. URL <https://doi.org/10.48550/arXiv.2502.09622>.

Guo, D., Yang, D., Zhang, H., Song, J., Wang, P., Zhu, Q., Xu, R., Zhang, R., Ma, S., Bi, X., et al. Deepseek-r1 incentivizes reasoning in llms through reinforcement learning. *Nature*, 645(8081):633–638, 2025.

He, G., Nie, S., Zhu, F., Zhao, Y., Bai, T., Yan, R., Fu, J., Li, C., and Yuan, B. Ultrallada: Scaling the context length to 128k for diffusion large language models. *CoRR*, abs/2510.10481, 2025.

Kim, J., Lee, C. K., Domingo-Enrich, C., Du, Y., Kakade, S. M., Ngotiaoco, T., Chen, S., and Albergo, M. S. Any-order flexible length masked diffusion. *CoRR*, abs/2509.01025, 2025.

Li, J., Dong, X., Zang, Y., Cao, Y., Wang, J., and Lin, D. Beyond fixed: Training-free variable-length denoising for diffusion large language models, 2025. URL <https://arxiv.org/abs/2508.00819>.

Li, X. L., Thickstun, J., Gulrajani, I., Liang, P., and Hashimoto, T. B. Diffusion-lm improves controllable text generation. In Koyejo, S., Mohamed, S., Agarwal, A., Belgrave, D., Cho, K., and Oh, A. (eds.), *Advances in Neural Information Processing Systems 35: Annual Conference on Neural Information Processing Systems 2022, NeurIPS 2022, New Orleans, LA, USA, November 28 - December 9, 2022*, 2022.

Lightman, H., Kosaraju, V., Burda, Y., Edwards, H., Baker, B., Lee, T., Leike, J., Schulman, J., Sutskever, I., and Cobbe, K. Let’s verify step by step. In *The Twelfth International Conference on Learning Representations, ICLR 2024, Vienna, Austria, May 7-11, 2024*. OpenReview.net, 2024. URL <https://openreview.net/forum?id=v8L0pN6EOi>.

Nie, S., Zhu, F., You, Z., Zhang, X., Ou, J., Hu, J., Zhou, J., Lin, Y., Wen, J.-R., and Li, C. Large language diffusion models, 2025. URL <https://arxiv.org/abs/2502.09992>.

Song, Y., Liu, X., Li, R., Liu, Z., Huang, Z., Guo, Q., He, Z., and Qiu, X. Sparse-dllm: Accelerating diffusion llms with dynamic cache eviction. *CoRR*, abs/2508.02558, 2025.

Wu, Z., Zheng, L., Xie, Z., Ye, J., Gao, J., Feng, Y., Li, Z., W., V., Zhou, G., and Kong, L. Dreamon: Diffusion language models for code infilling beyond fixed-size canvas, 2025. URL <https://hkunlp.github.io/blog/2025/dreamon>.

Xie, Z., Ye, J., Zheng, L., Gao, J., Dong, J., Wu, Z., Zhao, X., Gong, S., Jiang, X., Li, Z., and Kong, L. Dream-coder 7b: An open diffusion language model for code. *CoRR*, abs/2509.01142, 2025.

Xiong, Z., Cai, Y., Li, Z., and Wang, Y. Unveiling the potential of diffusion large language model in controllable generation. *CoRR*, abs/2507.04504, 2025.

Yadav, D. and Mondal, S. Evaluating pre-trained large language models on zero shot prompts for parallelization of source code. *J. Syst. Softw.*, 230:112543, 2025.

Yang, A., Li, A., Yang, B., Zhang, B., Hui, B., Zheng, B., Yu, B., Gao, C., Huang, C., Lv, C., et al. Qwen3 technical report. *arXiv preprint arXiv:2505.09388*, 2025a.

Yang, Y., Wang, C., Wang, S., Wen, Z., Qi, B., Xu, H., and Zhang, L. Diffusion llm with native variable generation lengths: Let [eos] lead the way, 2025b. URL <https://arxiv.org/abs/2510.24605>.

Ye, J., Xie, Z., Zheng, L., Gao, J., Wu, Z., Jiang, X., Li, Z., and Kong, L. Dream 7b: Diffusion large language models. *arXiv preprint arXiv:2508.15487*, 2025.

Zhang, A., Sivakumar, A., Tang, C., and Thomas, C. Flexible-length text infilling for discrete diffusion models. *CoRR*, abs/2506.13579, 2025a.

Zhang, Y., Ni, B., Chen, X.-S., Zhang, H.-R., Rao, Y., Peng, H., Lu, Q., Hu, H., Guo, M.-H., and Hu, S.-M. Bee: A high-quality corpus and full-stack suite to unlock advanced fully open mllms, 2025b. URL <https://arxiv.org/abs/2510.13795>.

Zhu, F., Wang, R., Nie, S., Zhang, X., Wu, C., Hu, J., Zhou, J., Chen, J., Lin, Y., Wen, J., and Li, C. Llada 1.5: Variance-reduced preference optimization for large language diffusion models. *CoRR*, abs/2505.19223, 2025a.

Zhu, F., You, Z., Xing, Y., Huang, Z., Liu, L., Zhuang, Y., Lu, G., Wang, K., Wang, X., Wei, L., Guo, H., Hu, J., Ye, W., Chen, T., Li, C., Tang, C., Feng, H., Hu, J., Zhou, J., Zhang, X., Lan, Z., Zhao, J., Zheng, D., Li, C., Li, J., and Wen, J. Llada-moe: A sparse moe diffusion language model. *CoRR*, abs/2509.24389, 2025b.

Table 6. Unified decoding configuration used across benchmarks. All results for LR-DLLM and baselines are obtained under the same settings unless otherwise noted.

Benchmark	Top- p	Top- k	Temperature
HumanEval-Infilling	0.9	None	0.2
McEval	0.9	None	0.2
MATH500	0.9	None	0.2
GSM8K	0.9	None	0.2
HumanEval	0.9	None	0.2

Model	Random Span (\pm std)	Single-line (\pm std)	Multi-line (\pm std)
LLaDA-8B	19.2 ± 0.1	69.4 ± 0.3	35.9 ± 0.2
LLaDA-1.5	20.5 ± 0.2	68.9 ± 0.2	34.6 ± 0.4
LLaDA-MoE	21.5 ± 0.1	71.3 ± 0.3	41.4 ± 0.4
Dream-7B	19.6 ± 0.2	76.7 ± 0.4	46.3 ± 0.2
DreamCoder-7B	23.2 ± 0.2	81.6 ± 0.3	53.8 ± 0.4

Table 7. Run-to-run variability of LR-DLLM on HumanEval-Infilling. We report the standard deviation of Pass@1 across N independent runs (different random seeds) for each setting.

A. Experimental Setup and Details

Baseline availability and coverage. We compare against representative variable-length diffusion baselines when their public releases allow reproducible evaluation under our settings. However, some contemporary methods cannot be uniformly evaluated across backbones due to limitations in released checkpoints and implementation availability. **DreamOn** (Wu et al., 2025) is only publicly released with DreamCoder checkpoints, and training the full system from scratch is computationally expensive (e.g., requiring large-scale multi-GPU training as reported by the authors); therefore, we report DreamOn comparisons only on the DreamCoder backbone. **FlexMDM** (Kim et al., 2025) does not provide public code at the time of writing; we thus cite the numbers reported in the original paper, noting that the paper reports results only for a limited subset of settings. Finally, **DAEDAL** (Li et al., 2025) is designed around the LLaDA family and is not directly applicable to Dream under its current framework; hence, we include DAEDAL only in the settings where it is compatible. Across all reported comparisons, we align inference budgets and evaluation protocols as closely as possible to ensure fairness, and we explicitly mark settings that are not applicable or not available.

Decoding and inference configuration. Unless otherwise specified, all experiments use the same decoding configuration for fair comparison. Specifically, we apply standard LLM sampling with nucleus sampling probability $p=0.9$, no top- k truncation, and temperature 0.2 across all benchmarks. The same decoding settings are used for LR-DLLM and all baseline methods whenever applicable. All reported results are obtained under fixed random seeds and deterministic decoding settings. We observed negligible variance across repeated runs (<0.5 Pass@1 on HumanEval-Infilling).

B. Run-to-Run Variability Analysis

Across all models and infilling settings, the run-to-run variability of LR-DLLM remains consistently small. As shown in Table 7, the standard deviation of Pass@1 is below 0.5 in all cases, indicating that the observed performance gains are not driven by stochastic fluctuations across runs. This stability holds across heterogeneous backbones and span regimes, suggesting that the proposed length-regularized inference yields reliable length decisions rather than exhibiting brittle or oscillatory behavior.

In particular, the magnitude of variability is an order of magnitude smaller than the absolute improvements reported in the main results, confirming that the benefits of LR-DLLM are stable rather than within noise.

Table 8. Comparison between fixed-length infilling with different mask sizes and LR-DLLM on HumanEval-Infilling using the DreamCoder backbone. We report Pass@1 accuracy (%).

Benchmark	Fixed Mask Length					LR-DLLM
	4	8	16	32	64	
Single-Line	24.9	61.2	72.6	62.4	55.5	81.6
Multi-Line	5.5	14.7	27.1	39.4	43.2	53.8

C. Clarification on Task-Agnosticity

In this paper, the term *task-agnostic* refers to the *structural generality* of the proposed inference framework, rather than empirical validation across all possible task categories. Specifically, LR-DLLM operates on a generic prefix–suffix composition $\mathbf{x} = \mathbf{p} \parallel \mathbf{y} \parallel \mathbf{s}$ and does not rely on task-specific supervision, loss functions, or architectural modifications.

In practice, this formulation subsumes two broad and commonly used generation paradigms: (i) *prefix–suffix infilling* (FIM), where both \mathbf{p} and \mathbf{s} are non-empty, and (ii) *left-to-right continuation*, which is recovered as the special case $\mathbf{s} = \emptyset$. Our empirical evaluation focuses on representative tasks within these paradigms, including code completion, multi-line infilling, and mathematical reasoning, which naturally instantiate the above structure.

We do not claim that LR-DLLM has been empirically validated on all task families (e.g., dialogue, summarization, or instruction following). Rather, the task-agnostic claim is intended in the sense that the method is *not specialized to any particular task*, and can in principle be applied to any generation problem that can be cast into a prefix–suffix composition with unknown span length.

D. Fixed-Length Mask Sweep on HumanEval-Infilling

Setup. We evaluate fixed-length infilling on HumanEval-Infilling using the DreamCoder backbone by sweeping the mask length $L \in \{4, 8, 16, 32, 64\}$ under identical inference budgets and decoding settings. Pass@1 accuracy is reported separately for Single-Line and Multi-Line infilling. Table 8 summarizes the numerical results, and Figure 4 visualizes the performance trends.

Results. As shown in Table 8, fixed-length performance exhibits a strong dependence on the chosen mask length. For Single-Line infilling, accuracy peaks at 72.6% with $L=16$ and degrades for larger masks (e.g., 62.4% at $L=32$ and 55.5% at $L=64$). For Multi-Line infilling, performance improves with increasing L up to 43.2% at $L=64$ but remains substantially below LR-DLLM (53.8%). Across both settings, LR-DLLM consistently outperforms the best fixed-length choice selected in hindsight (Table 8), indicating that its gains cannot be attributed solely to increasing MAX_LENGTH.

While ground-truth span lengths are available for HumanEval-Infilling, we focus on downstream correctness as the primary criterion, since multiple lengths may admit semantically valid solutions. Direct length error metrics (e.g., MAE) are therefore not fully aligned with task success.

E. Length-Induced Entropy in FIM and Continuation

In both fill-in-the-middle (FIM) and standard left-to-right continuation, we consistently observe a systematic trend: as the “free” generation region becomes longer, token predictions become less certain, and uncertainty tends to increase as tokens move farther away from the anchoring context (i.e., the boundary between conditioned and unconditioned spans). This phenomenon suggests that measured uncertainty contains an intrinsic length-dependent component in addition to the model’s quality-dependent component.

A statistical-physics view. We model this effect using the classical relation between entropy and the number of admissible microstates:

$$S = k \log N, \quad (8)$$

where N denotes the number of feasible configurations under macroscopic constraints and k is a constant scale factor. In language generation, macroscopic constraints are induced by the given context (prefix/suffix, syntax, semantics), while

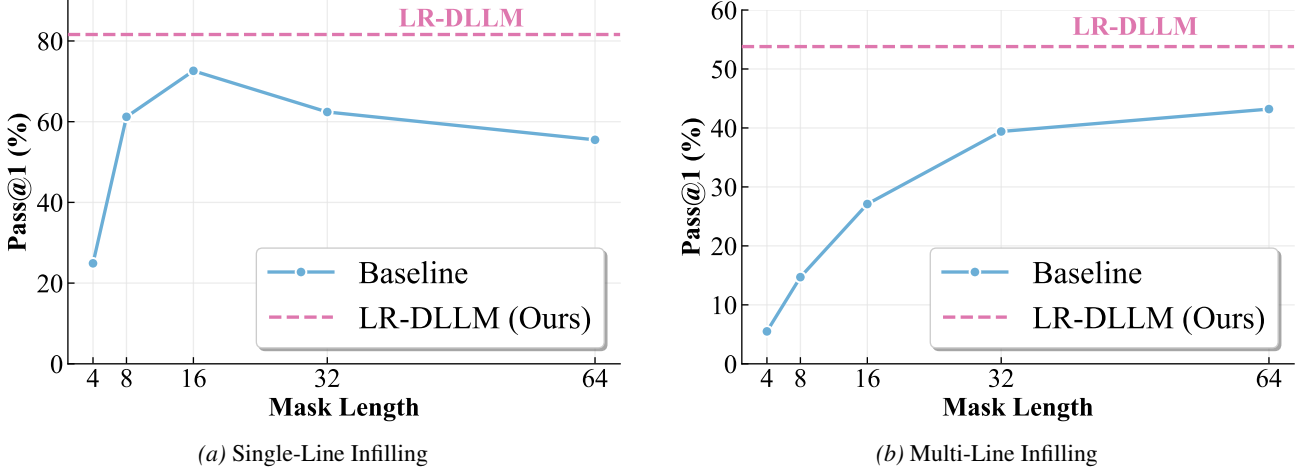


Figure 4. Effect of fixed mask length on HumanEval-Infilling. Solid lines denote fixed-length infilling with different mask sizes, while the dashed horizontal line corresponds to LR-DLLM.

microstates correspond to distinct valid token (or sequence) realizations consistent with those constraints.

Assumption: admissible choices increase with distance from the anchor. Consider a contiguous free region of length L . Index positions by their distance $d \in \{1, 2, \dots, L\}$ from an anchoring point.¹ We assume the effective number of admissible choices at distance d grows as a power law:

$$\#\text{choices}(d) \propto d^r, \quad r > 0, \quad (9)$$

capturing the intuition that contextual constraints weaken with distance.

Total number of configurations. Using a multiplicative approximation across positions, the number of feasible configurations for a length- L free region scales as

$$N(L) \propto \prod_{d=1}^L d^r = (L!)^r. \quad (10)$$

Length-induced entropy and its $\log L$ growth. Substituting Eq. (10) into Eq. (8), the entropy induced purely by the growth of admissible configurations with L is

$$S_2(L) = k \log N(L) \approx k \log(L!)^r = kr \log(L!). \quad (11)$$

Applying Stirling's approximation,

$$\log(L!) = L \log L - L + O(\log L), \quad (12)$$

we obtain the leading-order behavior

$$S_2(L) \approx kr(L \log L - L) \sim kr L \log L. \quad (13)$$

Define the average (per-token) length-induced entropy:

$$\overline{S}_2(L) := \frac{S_2(L)}{L} \approx kr \log L - kr + O\left(\frac{\log L}{L}\right). \quad (14)$$

Hence, up to an additive constant,

$$\overline{S}_2(L) \approx a \log L + b, \quad \text{with } a \approx kr. \quad (15)$$

This predicts that even with a fixed model, average predictive uncertainty should increase approximately linearly in $\log L$ as the free region grows.

¹For FIM, one may interpret d as the distance to the nearest boundary (prefix or suffix). The analysis below focuses on the dependence on L and thus applies qualitatively to both settings.

Decomposition: length effect vs. model quality. Let $\text{AVG_S}(L)$ denote a measurable average uncertainty statistic (e.g., average token entropy computed from model logits) at free length L . We decompose it as

$$\text{AVG_S}(L) = S_1(L) + \overline{S_2}(L), \quad (16)$$

where $\overline{S_2}(L)$ captures the inevitable length-induced contribution characterized above, and $S_1(L)$ is a quality-related term reflecting the model’s effective certainty under the current constraints.

Practical estimation via log-length fitting. Although $S_1(L)$ is not directly observable, $\text{AVG_S}(L)$ is measurable and $\overline{S_2}(L)$ admits the log-length form in Eq. (15). We therefore fit

$$\widehat{S_2}(L) = a \log L + b, \quad (17)$$

by regressing measured $\text{AVG_S}(L)$ over a small set of geometrically spaced lengths, e.g.,

$$L \in \{\text{MAX}, \text{MAX}/2, \text{MAX}/4, \dots\}. \quad (18)$$

We then estimate the quality-related component as

$$\widehat{S_1}(L) = \text{AVG_S}(L) - \widehat{S_2}(L). \quad (19)$$

Interpretation. The estimate $\widehat{S_1}(L)$ serves as a length-normalized uncertainty signal: it subtracts the predictable entropy growth attributable to increased free length, making uncertainty more comparable across different candidate lengths in both FIM and continuation settings.

F. Forward-Pass Complexity of LR-DLLM

We analyze the complexity of LR-DLLM in terms of the number of model forward evaluations. We count one *forward evaluation* as a single invocation of the DLLM inference procedure on a template $\mathbf{x}^{(0)}(L) = \mathbf{p} \parallel \langle \text{mask} \rangle^L \parallel \mathbf{s}$, which returns $\text{AVG}_{\text{conf}}(L; \mathbf{p}, \mathbf{s})$ (and the associated token distributions).

Stage I (exponential probing). Stage I evaluates $\text{AVG}_{\text{conf}}(L; \mathbf{p}, \mathbf{s})$ on the exponentially spaced set $\mathcal{L}_{\text{exp}} = \{1, 2, 4, \dots, 2^m\}$ where $2^m \leq L_{\text{max}}$. Thus Stage I uses

$$F_{\text{I}} = |\mathcal{L}_{\text{exp}}| = \lfloor \log_2 L_{\text{max}} \rfloor + 1 = O(\log L_{\text{max}}) \quad (20)$$

forward evaluations.

Stage II (greedy local search). At each commitment step $t \in \{1, \dots, N\}$, the algorithm performs greedy hill-climbing over lengths by comparing CL on neighboring lengths $\{L - 1, L, L + 1\}$, and then commits one token once a strict local maximum is reached. Let u_t denote the number of length updates (moves) performed before the t -th commitment.

Lemma F.1 (Monotonicity of the length search). *Within a fixed commitment step (i.e., with \mathbf{p}, \mathbf{s} held fixed), the greedy update rule never revisits a previous length. Hence, the length trajectory is monotone and terminates at a local maximum.*

Proof sketch. Suppose the algorithm moves from L to $L + 1$. By definition, $\text{CL}(L + 1) > \text{CL}(L)$. At the next iteration (still under the same context), L is a neighbor of $L + 1$, so moving back would require $\text{CL}(L) > \text{CL}(L + 1)$, contradicting the strict improvement. The same argument holds for moves to $L - 1$. \square

Counting forward evaluations in Stage II. At the beginning of each commitment step, we evaluate CL at $\{L - 1, L, L + 1\}$, requiring at most 3 forwards. By Lemma F.1, each move changes L by ± 1 and introduces at most one new boundary length whose CL has not been evaluated yet; therefore each additional move costs at most one forward evaluation. Moreover, in our implementation the inference outputs at the locally optimal length are reused to commit the token, so no extra forward is needed for commitment.² Therefore, the total number of forward evaluations in Stage II satisfies

$$F_{\text{II}} \leq \sum_{t=1}^N (3 + u_t) = 3N + U, \quad \text{where } U := \sum_{t=1}^N u_t. \quad (21)$$

²If an additional forward is used to commit, it only changes constants.

Worst-case upper bound. Since the length is always within $[1, L_{\max}]$, we have $u_t \leq L_{\max} - 1$ and hence $U \leq N(L_{\max} - 1)$. Plugging into Eq. (21) yields

$$F_{\text{II}} = O(NL_{\max}). \quad (22)$$

When $L_{\max} = O(N)$, this gives the conservative worst-case bound $F_{\text{II}} = O(N^2)$.

A tighter bound under a stability assumption. Let L_t^* denote the (strict) local maximizer reached at commitment step t under the corresponding context. Since we always initialize step t from the previous locally optimal length after committing one token, we have $L_t^{\text{init}} = L_{t-1}^* - 1$ for $t \geq 2$. By Lemma F.1, the number of moves is exactly the distance to the new local optimum:

$$u_t = |L_t^* - L_t^{\text{init}}| = |L_t^* - (L_{t-1}^* - 1)| \leq 1 + |L_t^* - L_{t-1}^*|. \quad (23)$$

Summing over t gives

$$U \leq N + \sum_{t=2}^N |L_t^* - L_{t-1}^*|. \quad (24)$$

Assumption F.2 (Bounded drift of locally optimal lengths). The locally optimal length does not change abruptly across successive subproblems, i.e., $\sum_{t=2}^N |L_t^* - L_{t-1}^*| = O(NH)$ for some H .

Under Assumption F.2, Eq. (24) implies $U = O(NH)$, and therefore Eq. (21) yields

$$F_{\text{II}} = O(NH). \quad (25)$$

In particular, if the drift satisfies $H = O(\log L_{\max})$ (or if $|L_t^* - L_{t-1}^*| \leq c \log L_{\max}$ uniformly), then

$$F_{\text{II}} = O(N \log L_{\max}). \quad (26)$$

Overall bound. Combining Stage I and Stage II, the total number of forward evaluations is

$$F_{\text{total}} = F_{\text{I}} + F_{\text{II}} = O(\log L_{\max}) + O(NL_{\max}) \quad (27)$$

in the worst case, and

$$F_{\text{total}} = O(\log L_{\max}) + O(NH) \quad (28)$$

under Assumption F.2. In practice, we observe that H is small, so the empirical complexity is close to linear.

G. Forward-Call Efficiency Distribution Across Models

We quantify the inference-time overhead of LR-DLLM using the ratio `Forward Calls`/`Generated Tokens`, where `Forward Calls` counts the number of model invocations used to evaluate $\text{AVG}_{\text{conf}}(L)$ (and thus $\text{CL}(L)$) during Stage I probing and Stage II local length search, and `Generated Tokens` is the number of committed tokens produced by Stage II. Figure 5 visualizes the per-instance distribution of this ratio for three backbones (**Dream**, **DreamCoder**, and **LLaDA-8B**) under an identical plotting protocol, while Table 9 reports summary statistics.

Across all three models, the distributions are markedly right-skewed: the median is consistently lower than the mean (e.g., Dream: 3.43 vs. 3.66; DreamCoder: 4.00 vs. 4.89; LLaDA-8B: 4.63 vs. 5.12), indicating that most instances incur a stable and moderate overhead, while a small number of hard cases forms a long tail and inflates the mean. Using the median as a robust measure of typical behavior, Dream is the most efficient backbone (median 3.43), followed by DreamCoder (median 4.00) and LLaDA-8B (median 4.63). The tails differ more substantially: Dream exhibits the tightest distribution (P95 = 5.00), whereas DreamCoder shows the heaviest tail (P95 = 11.23), with LLaDA-8B in between (P95 = 8.00). All three models have rare extreme outliers (max around 28–33), which are far beyond their respective P95 values, suggesting that they occur infrequently but can arise when many local length updates are triggered for instances with short effective generations or unstable local optima.

Overall, these results corroborate that, despite a conservative worst-case bound, LR-DLLM typically converges in only a few local updates per committed token on standard benchmarks, leading to a modest overhead for the vast majority of instances.

Table 9. Summary statistics of the per-instance ratio Forward Calls/Generated Tokens computed from generation logs (lower is better). Here Forward Calls counts model invocations used to evaluate $\text{AVG}_{\text{conf}}(L)$ (hence $\text{CL}(L)$) during Stage I and Stage II, and Generated Tokens is the number of committed tokens.

Model	n	Mean	Median	P95	Min	Max
Dream	1033	3.6574	3.4286	5.0000	2.0625	32.8333
DreamCoder	1033	4.8910	4.0000	11.2268	2.8594	27.6667
LLaDA-8B	1033	5.1211	4.6316	8.0000	2.7288	31.1429

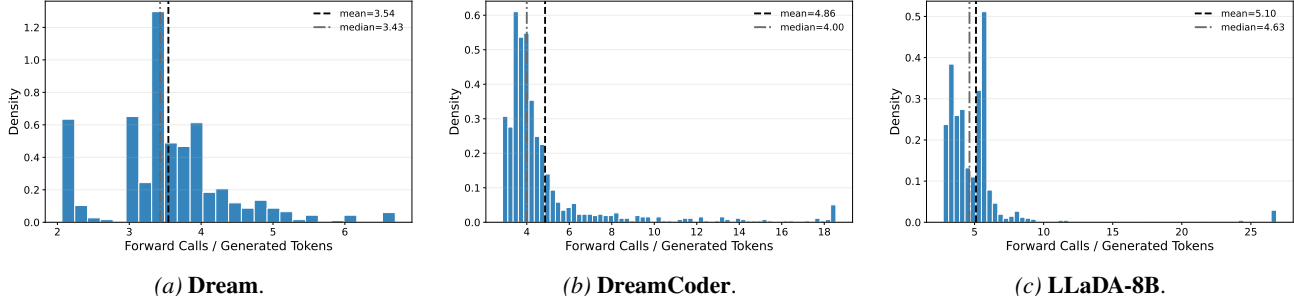


Figure 5. Per-instance distributions of the overhead ratio Forward Calls/Generated Tokens for three backbones under the same inference and logging protocol. Forward Calls counts model invocations used to evaluate $\text{AVG}_{\text{conf}}(L)$ (and thus $\text{CL}(L)$) during Stage I probing and Stage II greedy local length search, and Generated Tokens is the number of committed tokens produced by Stage II. The right-skewed shapes indicate a stable typical overhead with a small number of hard outliers.

H. Additional Comparison with dLLM-Var

We include an auxiliary comparison with dLLM-Var, a representative *training-based* variable-length method for diffusion LLMs. We do *not* report it in the main tables because its current public release is limited to a single trained checkpoint (LLADA-8B-Instruct) and a specific inference variant (block diffusion), and it only supports one-sided (backward-only) length growth. These constraints prevent a consistent evaluation across the multiple backbones and general prefix–suffix FIM settings considered in this paper. Nevertheless, for completeness, we report results on the subset of benchmarks that dLLM-Var can be evaluated on. For a fair comparison, we use the same maximum probing length $\text{MAX_LENGTH} = 256$ for LR-DLLM in all experiments below.

Discussion. Table 10 shows that LR-DLLM consistently outperforms dLLM-Var on the supported subset. Concretely, LR-DLLM improves GSM8K accuracy from 70.9 to 75.1 (+4.2 points), more than doubles performance on MATH500 from 18.4 to 39.8 (+21.4 points), and boosts HumanEval Pass@1 from 17.7 to 31.7 (+14.0 points). These gains are achieved while remaining training-free and model-agnostic, whereas dLLM-Var is tied to a specific trained LLADA-8B-Instruct checkpoint and a block-diffusion procedure with one-sided length growth. More importantly, LR-DLLM supports *bidirectional* length adjustment (both expansion and contraction) under general constrained generation, which is essential for prefix–suffix FIM and settings with large length variance. A broader open-source release of dLLM-Var covering more backbones and more general constrained generation settings would enable a more comprehensive comparison in future work.

I. Other Related Work

Several recent works have explored diffusion-based language models (DLLMs) from complementary perspectives. **UltraLLaDA** (He et al., 2025) focuses on extending the context window of DLLMs to very long sequences (up to 128K tokens), addressing scalability in context length rather than the inference-time determination of unknown span length. **Diffusion-LM** (Li et al., 2022) and **S3** (Xiong et al., 2025) demonstrate that diffusion-based formulations can be advantageous for conditional generation, but they operate under fixed-length generation assumptions and do not address variable-length inference.

Other works investigate efficiency and decoding acceleration for DLLMs. **DPad** (Chen et al., 2025) and **Sparse-dLLM** (Song et al., 2025) study architectural and systems-level optimizations, such as attention sparsification and KV-cache management, to improve inference speed. These methods are orthogonal to our focus, as they assume a predetermined generation length and do not consider length selection as part of the inference process.

Table 10. Comparison with dLLM-Var on the *restricted* subset of settings supported by its public release. dLLM-Var is only available as a trained LLADA-8B-Instruct checkpoint with block-diffusion inference and backward-only length growth; therefore it cannot be applied to other diffusion backbones or general prefix-suffix FIM requiring bidirectional length adjustment. We report LR-DLLM on the same backbone under training-free inference.

Benchmark	dLLM-Var	LR-DLLM
GSM8K (Acc.)	70.9	75.1
MATH500 (Acc.)	18.4	39.8
HumanEval (Pass@1)	17.7	31.7

Finally, **Theoretical Benefit and Limitation of Diffusion Language Models** (Feng et al., 2025) analyzes fundamental challenges of DLLMs, explicitly noting the difficulty of variable-length generation. Our work is complementary in that it directly targets this limitation by introducing an inference-time framework for adaptive length determination, without modifying the underlying model or training procedure.

J. Case Study

J.1. Infilling

Python Infilling Example

```
def string_transformation(A: str, B: str, rules: list) -> Union[int, str]:
    queue = deque([(A, 0)])  # Each element in the queue is a tuple (current_string, steps_taken)
    visited = set([A])  # Keep track of visited strings to avoid loops

    # Perform BFS
    while queue:
        current, steps = queue.popleft()
        if current == B:
            return steps
        #BEGIN INFILLING
        for source, target in rules:
            new_current = current.replace(source, target)
            if new_current not in visited:
                visited.add(new_current)
                queue.append((new_current, steps + 1))
        #END INFILLING
    return "NO ANSWER!"
```

C++ Infilling Example

```
int countPermutations(int n, int k, int qq[])
{
    const int N = 505, P = 998244353;
    int q[N], m, dp[N][N], jc[N], f[N], ans;

    memset(q, 0, sizeof(q));
    memset(dp, 0, sizeof(dp));
    memset(jc, 0, sizeof(jc));
    memset(f, 0, sizeof(f));
    ans = 0;

    for (int i = 1; i <= n; i++)
        q[i] = qq[i - 1];

    dp[0][0] = f[0] = 1;
    ## START INFILLING
    for (int i = 1; i <= n; i++)
    {
        f[i] = f[i - 1];
    }

    for (int i = 1; i <= n; i++)
```

```

{
    for (int j = 0; j < i; j++)
        for (int k = 1; k <= n; k++)
            dp[i][k] = (dp[i][k] + dp[j][k - 1] * 1LL * f[i - j] % P) % P;
}
## END INFILLING
m = 0;
for (int i = 1; i <= n; i++)
    if (q[i] > q[i + 1])
    {
        m = i;
        break;
    }

if (m == n)
{
    for (int i = k; i <= n; i++)
        ans = (ans + dp[n][i]) % P;
}
else
{
    for (int i = m + 1; i <= n; i++)
    {
        if (i != m + 1 && (q[i - 1] > q[i] || q[i] < q[m]))
            break;

        int c = k + i - n - 1;
        if (c >= 0)
            ans = (ans + dp[m][c] * 1LL * jc[i - m - 1] % P) % P;
    }
}

return ans;
}
}

```

J.2. Completion

Math Completion Example

Question:

What is the least positive integer multiple of 30 that can be written with only the digits 0 and 2?

Answer:

To find the least positive integer multiple of 30 that can be written with only the digits 0 and 2, we need to follow these steps:

1. **Identify the properties of multiples of 30:** - A number is a multiple of 30 if it is divisible by both 3 and 10. - A number is divisible by 3 if the sum of its digits is divisible by 3. - A number is divisible by 10 if its last digit is 0.
2. **Form the smallest number using the digits 0 and 2:** - The smallest number we can form using the digits 0 and 2 is 20.

3. **Check if 20 is a multiple of 30:** - The sum of the digits of 20 is

$$(2 + 0 = 2)$$

, which is not divisible by 3. - The last digit of 20 is 0, so it is divisible by 10.

4. **Form the next smallest number:** - The next smallest number we can form using the digits 0 and 2 is 220.

5. **Check if 220 is a multiple of 30:** - The sum of the digits of 220 is

$$(2 + 2 + 0 = 4)$$

, which is not divisible by 3. - The last digit of 220 is 0, so it is divisible by 10.

6. **Form the next smallest number:** - The next smallest number we can form using the digits 0 and 2 is 2220.

7. **Check if 2220 is a multiple of 30:** - The sum of the digits of 2220 is

$$(2 + 2 + 2 + 0 = 6)$$

, which is divisible by 3. - The last digit of 2220 is 0, so it is divisible by 10.

Since 2220 satisfies both conditions, it is the least positive integer multiple of 30 that can be written with only the digits 0 and 2.

Therefore, the answer is:

boxed{2220}

Code Completion Example

```
from typing import List\n\n\n\ndef rescale_to_unit(numbers: List[float]) -> List[float]:\n    """ Given list of numbers (of at least two elements), apply a linear transform to that list,\n    such that the smallest number will become 0 and the largest will become 1\n    >>> rescale_to_unit([1.0, 2.0, 3.0, 4.0, 5.0])\n    [0.0, 0.25, 0.5, 0.75, 1.0]\n    """\n    #Completion Start\n    if len(numbers) < 2:\n        raise ValueError(\"The list must contain at least two elements\")\n    min_val = min(numbers)\n    max_val = max(numbers)\n    return [(x - min_val) / (max_val - min_val) for x in numbers]
```